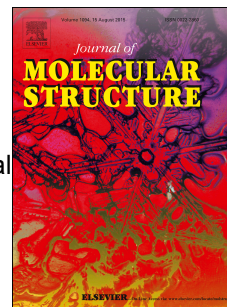


# Accepted Manuscript

Two families of bis(imido) symmetrical Schiff bases: X-ray crystal structure and optical properties

Xiao-Na Ma, Xue-Jie Tan, Dian-Xiang Xing, Qi-Cheng Sui, Jian-Min Liu, Chen-Xing Xu, Yun Liu



PII: S0022-2860(17)30241-7

DOI: [10.1016/j.molstruc.2017.02.082](https://doi.org/10.1016/j.molstruc.2017.02.082)

Reference: MOLSTR 23476

To appear in: *Journal of Molecular Structure*

Received Date: 24 January 2017

Revised Date: 21 February 2017

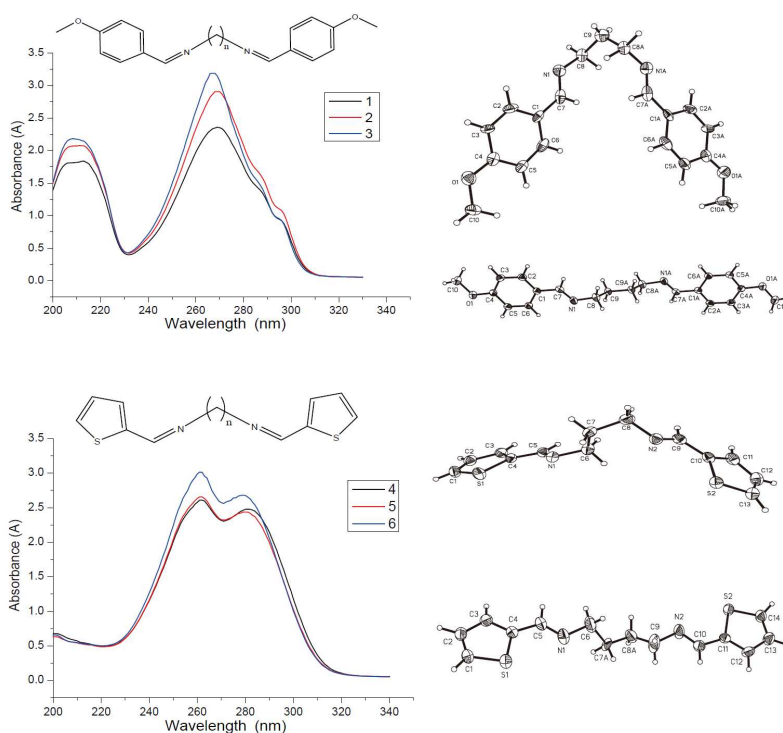
Accepted Date: 21 February 2017

Please cite this article as: X.-N. Ma, X.-J. Tan, D.-X. Xing, Q.-C. Sui, J.-M. Liu, C.-X. Xu, Y. Liu, Two families of bis(imido) symmetrical Schiff bases: X-ray crystal structure and optical properties, *Journal of Molecular Structure* (2017), doi: 10.1016/j.molstruc.2017.02.082.

This is a PDF file of an unedited manuscript that has been accepted for publication. As a service to our customers we are providing this early version of the manuscript. The manuscript will undergo copyediting, typesetting, and review of the resulting proof before it is published in its final form. Please note that during the production process errors may be discovered which could affect the content, and all legal disclaimers that apply to the journal pertain.

**Graphic Abstract:**

Two families of dimers provide longer alkyl bridges between two methoxy benzene rings and two thiophene rings (propane  $\rightarrow$  butane  $\rightarrow$  dodecane), while maintaining the same optical properties and the same spectroscopy mechanisms. Single crystal structures and DFT calculations were used to interpret their similarities and differences.



**Two families of bis(imido) symmetrical Schiff bases: X-ray crystal structure and optical properties**

Xiao-Na Ma <sup>a</sup>, Xue-Jie Tan <sup>a\*</sup>, Dian-Xiang Xing <sup>a</sup>, Qi-Cheng Sui <sup>a</sup>, Jian-Min Liu <sup>a</sup>, Chen-Xing Xu <sup>a</sup>, Yun Liu <sup>a</sup>

<sup>a</sup> School of Chemistry and Pharmaceutical Engineering, Qilu University of Technology, Jinan, Shandong Province, 250353, P. R. China.

**Abstract**

Two families of bis(imido) symmetrical Schiff bases based on 4-methoxybenzaldehyde and thiophene-2-carbaldehyde linked by three lengths of alkyl groups (propane → butane → dodecane) have been prepared and characterized by <sup>1</sup>H and <sup>13</sup>C NMR, Q-TOF mass spectroscopy, IR and elemental analysis. The structures and conformations of four of them have been established by X-ray single-crystal diffraction analysis. It is interesting that different linking groups and different conformations hardly have effect on several properties. For example, they have nearly the same melting points, the same UV-Vis absorption spectra and the same fluorescence emission spectra. Spectral interpretations were guided by time-dependent DFT calculated transition energies and oscillator strengths, which agree well with the experimental UV-Vis spectra. TD-DFT calculations reveal that they share nearly the same transition mechanism, *i. e.* both bands are largely originated from the  $\pi \rightarrow \pi^*$  transitions and have little or nothing to do with the alkyl bridge. However, there are also important differences based on the identity of the terminal groups. For example, similar dimers **1** and **2** crystallize in very different space groups  $P4_32_12$  (No. 96) and  $P2_1/n$  (No. 14), and another set of similar dimers **4** and **5** crystallize in  $P2_1/n$  (No. 14) and  $P2_12_12_1$  (No. 16), respectively. This illustrates the flexible nature of these dimers in forming a variety of different packing motifs. The results of this research suggest that the rational design and prediction of crystal structures are more difficult than optical properties, even though similar weak interactions can be controlled in assembling the molecules.

**1. Introduction**

Symmetry plays an important role in a variety of biological processes and the dimer structure is ubiquitous in natural products [1]. The dimeric molecules would be expected to show enhanced biological activity relative to their corresponding monomeric counterparts. [2] So dimeric compounds have been synthesized and studied for the treatment of cancer, HIV, Alzheimer, malaria and various parasitic diseases. [3] Besides medicinal science, organic dimers are also widely used in optoelectronic

<sup>a</sup> Corresponding author. E-mail: tanxuejie@163.com, Tel.: +86 531 89631208; fax: +86 531 89631207.

materials [4 and references therein], functional dye materials [5 and references therein] and supramolecular materials [6]. Recently, tethering two functional headgroups together with various bridging chains is being successfully used in designing functional materials following the concept of crystal engineering [7].

One key structural factor about dimer is the bridging group with different size, shape, length, and conformation. Expanded  $\pi$ -conjugated dimers such as ethynylene-conjugated porphyrin networks [8], phenyl dimers [9], pentacene dimers [10] and quinoidal bithiophene molecules [11] are of particular interest because of their excellent electronic coupling. While  $\pi$ -conjugated groups linked by more than one single bonds, by contrast, have much less been studied on the point of optical properties, for the lack of considerable electronic delocalization and therefore weakly exciton-coupling [12]. Of equal importance is their flexibility. Namely, as the length of the spacer increases, the more flexible nature of the dimer may allow it to freely bend and rotate, which may result in distinct structural topologies, intriguing conformations, diverse properties and packing structures. On one hand, the flexibility makes the rational design of clusters impossible at the current stage; on the other hand, the flexibility affords enough structural adaptability for more complicated designing. Dimers with  $-(\text{CH}_2)_n-$  ( $n \geq 3$ ) spacers are not well understood and there is an urgent need for more simple and flexible models without too much bias for certain conformations, which may provide different capacities of spatial extension and induce the construction of diverse frameworks.

As experimental evidence, the optical properties related to the electronic transition are important, useful yet simple indicator about the dimer structures. Herein, we report the synthesis, structures, and optical properties of two families of alkyl-linked bis(imido) symmetrical Schiff bases (can be called "Schiff base dimers" for clarity). As new flexible models for better understanding of the relationship between bridging groups, supramolecular arrangements and optical properties, precise crystal structure investigations have been carried out and theoretical calculations were used to elucidate the electronic transition mechanisms.

## 2. Experimental

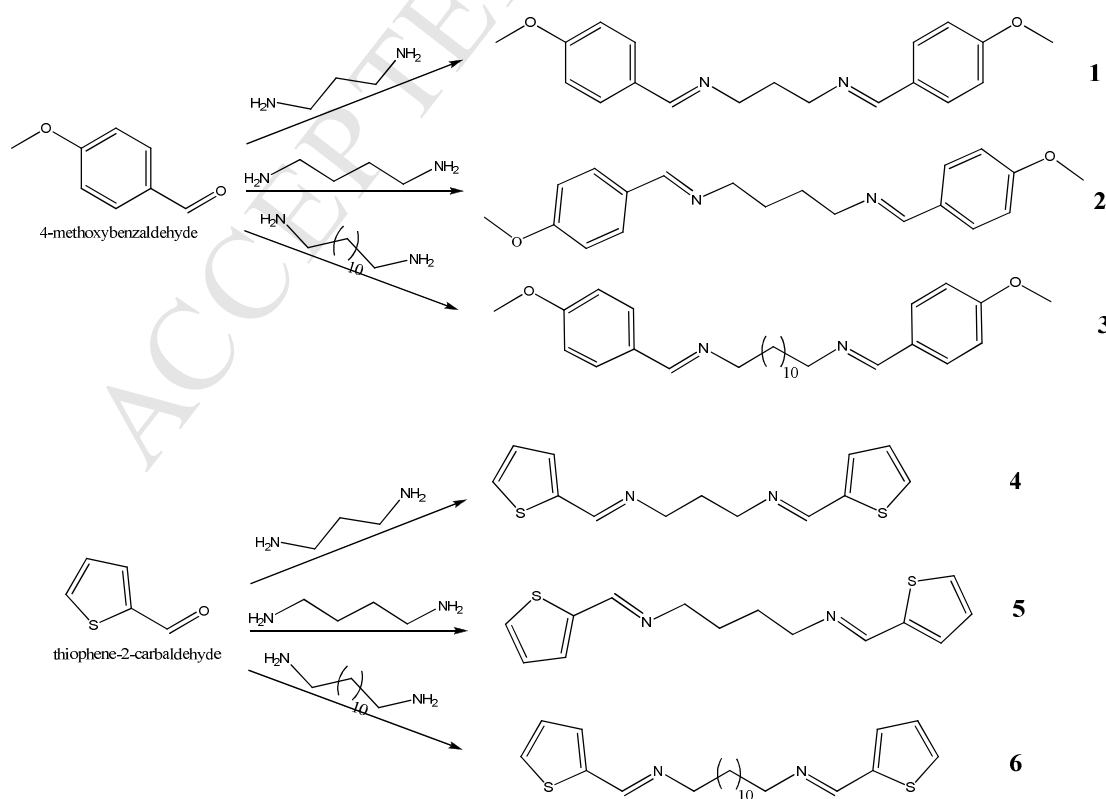
### 2.1. Materials and measurements

All chemicals were purchased from Aladdin-reagent Chemicals and were used without further purification. Elemental (C, H, N) analyses were carried out with a Perkin-Elmer 2400 microanalyzer.

Accurate-mass measurements were acquired on an Agilent-6520 quadrupole-time of flight tandem mass spectrometer, Q-TOF.  $^1\text{H}$  and  $^{13}\text{C}$  NMR spectra were run on a Bruker Avance 400 MHz instruments. The chemical shifts are reported in parts per million (ppm) relative to tetramethylsilane,  $\text{SiMe}_4$  ( $\delta = 0$  ppm), referenced to the chemical shifts of residual solvent peak [deuterated dimethyl sulfoxide (DMSO- $d_6$ )]. UV-Vis absorption spectra were recorded using a UV-1700 spectrophotometer (Shimadzu, Japan), in  $1 \times 10^{-5} \text{ mol} \cdot \text{L}^{-1}$  ethanol solution. Infrared (IR) spectra were obtained as KBr pellets with a Bruker tensor 27 FT-IR spectrometer (Bruker, Germany). Ensemble fluorescence spectra were performed on a HITACHI F-4600 fluorescence spectrophotometer (Hitachi Co. Ltd., Japan). Melting points were determined on a WRS-2A electrothermal digital melting point apparatus (Shanghai precision & scientific instrument Co., Ltd, China).

## 2.2. Synthesis and crystallization

All Schiff-base dimers were readily prepared by similar condensation reaction of the corresponding aldehydes (4-methoxybenzaldehyde and thiophene-2-carbaldehyde) with the diamines (trimethylenediamine, 1, 4-butanediamine and 1, 12-dodecanediamine) by refluxing for 1-3 h in absolute ethanol in a 2:1 mol ratio. After cooling, white flocculent or scale like precipitate was obtained (only dimer **6** is pale yellow), which on re-crystallization from ethanol gave colorless crystals suitable for X-ray analysis. But dimers based on 1, 12-dodecanediamine (dimers **3** and **6**) have a tendency to crystallize as fine powders. No crystal of sufficient thickness and quality could be obtained to perform a single-crystal analysis. The general reactions are shown in **Scheme 1**:



**Scheme 1.** Synthesis and structures of six Schiff-base dimers in this paper. Systematic names:

- 1, (N<sup>1</sup>E,N<sup>3</sup>E)-N<sup>1</sup>,N<sup>3</sup>-bis(4-methoxybenzylidene)propane-1,3-diamine;
- 2, (N<sup>1</sup>E,N<sup>4</sup>E)-N<sup>1</sup>,N<sup>4</sup>-bis(4-methoxybenzylidene)butane-1,4-diamine;
- 3, (N<sup>1</sup>E,N<sup>12</sup>E)-N<sup>1</sup>,N<sup>12</sup>-bis(4-methoxybenzylidene)dodecane-1,12-diamine;
- 4, (N<sup>1</sup>E,N<sup>3</sup>E)-N<sup>1</sup>,N<sup>3</sup>-bis(thiophen-2-ylmethylene)propane-1,3-diamine;
- 5, (N<sup>1</sup>E,N<sup>4</sup>E)-N<sup>1</sup>,N<sup>4</sup>-bis(thiophen-2-ylmethylene)butane-1,4-diamine;
- 6, (N<sup>1</sup>E,N<sup>12</sup>E)-N<sup>1</sup>,N<sup>12</sup>-bis(thiophen-2-ylmethylene)dodecane-1,12-diamine.

The physico-chemical characterization results are listed below. All NMR spectra are submitted as Supporting Information, see **Figs. S1-S12** (All “S” numbered tables and figures are in ESI):

**1** Elemental analysis: found (calc. for C<sub>19</sub>H<sub>22</sub>N<sub>2</sub>O<sub>2</sub>): C, 61.71 (61.75%); H, 4.96 (5.03%); N, 7.62 (7.57%); HRMS (ESI): *m/z* calcd for C<sub>19</sub>H<sub>22</sub>N<sub>2</sub>O<sub>2</sub>+H<sup>+</sup>: 311.1760 [*M*+H<sup>+</sup>]; found: 311.1764; M.p. 76.4-77.6°C [different from literatures: 79.0-79.5°C [13], 81°C [14], 81-82°C [15], 74-76°C [16], 78-80°C [17] ], <sup>1</sup>H NMR (DMSO): δ (ppm) 8.25 (s, 2H, imine protons, H-C=N), 7.67 (d, 4H, <sup>3</sup>J<sub>H-H</sub> = 8.4 Hz, phenyl protons), 6.98 (d, 4H, <sup>3</sup>J<sub>H-H</sub> = 8.4 Hz, phenyl protons), 3.78 (s, 6H, methoxy protons, CH<sub>3</sub>O-), 3.57 (t, 4H, <sup>3</sup>J<sub>H-H</sub> = 6.8 Hz, methylene protons, N-CH<sub>2</sub>-), 1.91 (m, 2H, <sup>3</sup>J<sub>H-H</sub> = 6.8 Hz, central methylene protons, -CH<sub>2</sub>-). <sup>13</sup>C NMR (DMSO): δ (ppm) 161.07 (phenyl carbons linked to methoxy groups), 160.00 (imine carbons, C=N), 129.29 (phenyl carbons linked to imine groups), 129.28 (phenyl carbons), 114.03 (phenyl carbons), 58.21 (methylene carbons, N-CH<sub>2</sub>-), 55.22 (methoxy carbons), 32.07 (central methylene carbons, -CH<sub>2</sub>-). FT-TR (cm<sup>-1</sup>, KBr): 3003 (w, ν C=C-H), 2945 (m, ν C-H), 2930 (m, ν C-H), 2833(m, ν C-H), 1638 (s, ν C=N), 1605 (s, ν C=N), 1308 (vs, ν C-O-C); UV/Vis (CH<sub>3</sub>CH<sub>2</sub>OH) λ<sub>max</sub>/nm (ε/L·mol<sup>-1</sup>·cm<sup>-1</sup>): 213.0 (1.8×10<sup>5</sup>), 269.0 (2.4×10<sup>5</sup>).

**2** Elemental analysis: found (calc. for C<sub>20</sub>H<sub>24</sub>N<sub>2</sub>O<sub>2</sub>): C, 74.16 (74.04%); H, 7.53 (7.46%); N, 8.75 (8.64%); HRMS (ESI): *m/z* calcd for C<sub>20</sub>H<sub>24</sub>N<sub>2</sub>O<sub>2</sub>+H<sup>+</sup>: 325.1916 [*M*+H<sup>+</sup>]; found: 325.1917; M.p. 76.6-77.2°C [different from literatures: 108-109°C [17], 105°C [18], 116-117°C [16], 117-118°C [19] ] <sup>1</sup>H NMR (DMSO): δ (ppm) 8.45 (s, 2H, imine protons, H-C=N), 7.67 (d, 4H, <sup>3</sup>J<sub>H-H</sub> = 8.4 Hz, phenyl protons), 6.98 (d, 4H, <sup>3</sup>J<sub>H-H</sub> = 8.4 Hz, phenyl protons), 3.78 (s, 6H, methoxy protons, CH<sub>3</sub>O-), 3.57 (t, 4H, <sup>3</sup>J<sub>H-H</sub> = 6.8 Hz, methylene protons, N-CH<sub>2</sub>-), 1.91 (m, 4H, <sup>3</sup>J<sub>H-H</sub> = 6.8 Hz, central methylene protons, -CH<sub>2</sub>-). <sup>13</sup>C NMR (DMSO): δ (ppm) 161.07 (phenyl carbons linked to methoxy groups), 159.99 (imine carbons, C=N), 129.20 (phenyl carbons linked to imine groups), 129.12 (phenyl carbons), 114.03 (phenyl carbons), 58.21 (methylene carbons, N-CH<sub>2</sub>-), 55.23 (methoxy carbons), 32.08 (central methylene carbons, -CH<sub>2</sub>-). FT-TR(cm<sup>-1</sup>, KBr): 3003 (w, ν C=C-H), 2945 (m, ν C-H), 2930 (m, ν C-H), 2837 (m, ν C-H), 1638 (s, ν C=N), 1605 (s, ν C=N), 1248 (vs, ν C-O-C); UV/Vis (CH<sub>3</sub>CH<sub>2</sub>OH)

$\lambda_{\text{max/nm}}$  ( $\epsilon/\text{L}\cdot\text{mol}^{-1}\cdot\text{cm}^{-1}$ ): 211.0 ( $2.1\times 10^5$ ), 268.0 ( $2.9\times 10^5$ ).

**3** Elemental analysis: found (calc. for  $\text{C}_{28}\text{H}_{40}\text{N}_2\text{O}_2$ ): C, 77.11 (77.02%); H, 9.28 (9.23%); N, 6.46 (6.42%). HRMS (ESI):  $m/z$  calcd for  $\text{C}_{28}\text{H}_{40}\text{N}_2\text{O}_2+\text{H}^+$ : 436.3090 [ $M+\text{H}^+$ ]; found: 436.3091. M.p. 76.8-77.0°C;  $^1\text{H}$  NMR (DMSO):  $\delta$  (ppm) 8.22 (s, 2H, imine protons, H-C=N), 7.64 (d, 4H,  $^3J_{\text{H-H}} = 8.4$  Hz, phenyl protons), 6.97 (d, 4H,  $^3J_{\text{H-H}} = 8.4$  Hz, phenyl protons), 3.77 (s, 6H, methoxy protons,  $\text{CH}_3\text{O}$ -), 3.48 (t, 4H,  $^3J_{\text{H-H}} = 6.4$  Hz, methylene protons, N- $\text{CH}_2$ -), 1.55 (d, 4H,  $^3J_{\text{H-H}} = 6.0$  Hz, methylene protons, - $\text{CH}_2$ -), 1.26-1.22 (d, 16H, methylene protons, - $\text{CH}_2$ -).  $^{13}\text{C}$  NMR (DMSO):  $\delta$  (ppm) 161.01(phenyl carbons linked to methoxy groups), 159.52 (imine carbons, C=N), 129.27 (phenyl carbons linked to imine groups), 129.04 (phenyl carbons), 113.96 (phenyl carbons), 60.40 (methylene carbons, N- $\text{CH}_2$ -), 55.22 (methoxy carbons), 30.51 (methylene carbons), 28.93 (methylene carbons), 28.73 (methylene carbons), 26.70 (methylene carbons). FT-TR( $\text{cm}^{-1}$ , KBr): 3071 (w,  $\nu$  C=C-H), 3003 (w,  $\nu$  C=C-H), 2920 (vs,  $\nu$  C-H), 2847 (s,  $\nu$  C-H), 1645 (s,  $\nu$  C=N), 1605 (s,  $\nu$  C=N), 1252 (vs,  $\nu$  C-O-C); UV/Vis ( $\text{CH}_3\text{CH}_2\text{OH}$ )  $\lambda_{\text{max/nm}}$  ( $\epsilon/\text{L}\cdot\text{mol}^{-1}\cdot\text{cm}^{-1}$ ): 208.0 ( $2.2\times 10^5$ ), 266.0 ( $3.2\times 10^5$ ).

**4** Elemental analysis: found (calc. for  $\text{C}_{13}\text{H}_{14}\text{N}_2\text{S}_2$ ): C, 59.66 (59.51%); H, 5.45 (5.38%); N, 10.76 (10.68%); HRMS (ESI):  $m/z$  calcd for  $\text{C}_{13}\text{H}_{14}\text{N}_2\text{S}_2+\text{H}^+$ : 263.0677 [ $M+\text{H}^+$ ]; found: 263.0679; M.p. 63.9-64.3°C [different from literatures: 36-38°C [20], 68°C [21], 40-41°C [22]].  $^1\text{H}$  NMR (DMSO):  $\delta$  (ppm) 8.45 (s, 2H, imine protons, H-C=N), 7.64 (d, 2H,  $^3J_{\text{H-H}} = 5.2$  Hz, thiophene protons), 7.44 (d, 2H,  $^3J_{\text{H-H}} = 3.6$  Hz, thiophene protons), 7.13 (t, 2H,  $^3J_{\text{H-H}} = 4.0$  Hz, thiophene protons), 3.55 (t, 4H,  $^3J_{\text{H-H}} = 6.8$  Hz, methylene protons, N- $\text{CH}_2$ -), 1.88 (m, 2H,  $^3J_{\text{H-H}} = 6.8$  Hz, central methylene protons, - $\text{CH}_2$ -).  $^{13}\text{C}$  NMR (DMSO):  $\delta$  (ppm) 154.65 (imine carbons, C=N), 142.31 (thiophene carbons linked to imine groups), 131.00 (thiophene carbons), 129.21 (thiophene carbons), 127.64 (thiophene carbons), 57.69 (methylene carbons, N- $\text{CH}_2$ -), 31.71 (central methylene carbons, - $\text{CH}_2$ -). FT-TR( $\text{cm}^{-1}$ , KBr): 3071 (w,  $\nu$  C=C-H), 3022 (w,  $\nu$  C=C-H), 2943 (m,  $\nu$  C-H), 2920 (m,  $\nu$  C-H), 2876 (m,  $\nu$  C-H), 2833 (m,  $\nu$  C-H), 1632 (vs,  $\nu$  C=N), 1429 (s,  $\nu$  C-S-C); UV/Vis ( $\text{CH}_3\text{CH}_2\text{OH}$ )  $\lambda_{\text{max/nm}}$  ( $\epsilon/\text{L}\cdot\text{mol}^{-1}\cdot\text{cm}^{-1}$ ): 261.0 ( $2.6\times 10^5$ ), 281.0 ( $2.5\times 10^5$ ).

**5** Elemental analysis: found (calc. for  $\text{C}_{14}\text{H}_{16}\text{N}_2\text{S}_2$ ): C, 60.98 (60.83%); H, 5.96 (5.83%); N, 10.27 (10.13%); HRMS (ESI):  $m/z$  calcd for  $\text{C}_{14}\text{H}_{16}\text{N}_2\text{S}_2+\text{H}^+$ : 277.0833 [ $M+\text{H}^+$ ]; found: 277.0833; M.p. 68.9-69.6°C [different from literature [21] 75°C].  $^1\text{H}$  NMR (DMSO):  $\delta$  (ppm) 8.44 (s, 2H, imine protons, H-C=N), 7.63 (d, 2H,  $^3J_{\text{H-H}} = 5.2$  Hz, thiophene protons), 7.42 (d, 2H,  $^3J_{\text{H-H}} = 3.2$  Hz, thiophene protons), 7.12 (t, 2H,  $^3J_{\text{H-H}} = 4.0$  Hz, thiophene protons), 3.52 (s, 4H, methylene protons, N- $\text{CH}_2$ -), 1.59 (s, 4H,

central methylene protons, -CH<sub>2</sub>-). <sup>13</sup>C NMR (DMSO): δ (ppm) 154.36 (imine carbons, C=N), 142.31 (thiophene carbons linked to imine groups), 130.98 (thiophene carbons), 129.18 (thiophene carbons), 127.67 (thiophene carbons), 59.75 (methylene carbons, N-CH<sub>2</sub>-), 28.16 (central methylene carbons, -CH<sub>2</sub>-). FT-TR(cm<sup>-1</sup>, KBr): 3078 (w, ν C=C-H), 2926 (s, ν C-H), 2860 (m, ν C-H), 2833 (m, ν C-H), 1630 (vs, ν C=N), 1429 (s, ν C-S-C); UV/Vis (CH<sub>3</sub>CH<sub>2</sub>OH) λ<sub>max</sub>/nm (ε/L·mol<sup>-1</sup>·cm<sup>-1</sup>): 261.0 (2.7×10<sup>5</sup>), 279.0 (2.4×10<sup>5</sup>).

**6** Elemental analysis: found (calc. for C<sub>22</sub>H<sub>32</sub>N<sub>2</sub>S<sub>2</sub>): C, 68.05 (67.99%); H, 8.39 (8.30%); N, 7.32 (7.21%); HRMS (ESI): *m/z* calcd for C<sub>22</sub>H<sub>32</sub>N<sub>2</sub>S<sub>2</sub>+H<sup>+</sup>: 388.2007 [*M*+H<sup>+</sup>]; found: 388.2007; M.p. 59.8-60.3°C. <sup>1</sup>H NMR (DMSO): δ (ppm) 8.42 (s, 2H, imine protons, H-C=N), 7.62 (d, 2H, <sup>3</sup>J<sub>H-H</sub> = 5.2 Hz, thiophene protons), 7.42 (d, 2H, <sup>3</sup>J<sub>H-H</sub> = 3.2 Hz, thiophene protons), 7.11 (t, 2H, <sup>3</sup>J<sub>H-H</sub> = 4.0 Hz, thiophene protons), 3.47 (t, 4H, <sup>3</sup>J<sub>H-H</sub> = 6.8 Hz, methylene protons, N-CH<sub>2</sub>-), 1.54 (t, 4H, <sup>3</sup>J<sub>H-H</sub> = 6.4 Hz, methylene protons, -CH<sub>2</sub>-), 1.25-1.22 (d, 16H, methylene protons, -CH<sub>2</sub>-). <sup>13</sup>C NMR (DMSO): δ (ppm) 154.12 (imine carbons, C=N), 142.39 (thiophene carbons linked to imine groups), 130.81 (thiophene carbons), 129.07 (thiophene carbons), 127.61 (thiophene carbons), 59.98 (methylene carbons, N-CH<sub>2</sub>-), 30.32 (methylene carbons), 28.92 (methylene carbons), 28.70 (methylene carbons), 26.66 (methylene carbons). FT-TR(cm<sup>-1</sup>, KBr): 3096 (w, ν C=C-H), 3073 (w, ν C=C-H), 2918 (vs, ν C-H), 2849 (s, ν C-H), 1632 (vs, ν C=N), 1429 (m, ν C-S-C); UV/Vis (CH<sub>3</sub>CH<sub>2</sub>OH) λ<sub>max</sub>/nm (ε/L·mol<sup>-1</sup>·cm<sup>-1</sup>): 261.0 (3.0×10<sup>5</sup>), 279.0 (2.7×10<sup>5</sup>).

### 2.3 X-Ray Crystallographic Analysis

The X-ray diffraction measurements were made on a Bruker APEX II CCD area detector diffractometer at 293/298K for compounds **1**, **2** and **4**, **5** (Mo Kα radiation, graphite monochromator, λ = 0.71073 Å). The structures were solved by SHELXL-97. The absorption correction was done using the SADABS program. [23] Software packages APEX II (data collection), SAINT (cell refinement and data reduction), SHELXTL (data reduction, molecular graphics and publication material), DIAMOND (simplifying crystal packing diagram) were also used. [24-26] All non-hydrogen atoms were refined with anisotropic displacement parameters. Crystal data, data collection and structure refinement details are summarized in **Table 1**.

**Table 1** Crystallographic data and structure refinements summary for four dimers.

Compounds	<b>1</b>	<b>2</b>	<b>4</b>	<b>5</b>
Chemical formula	C <sub>19</sub> H <sub>22</sub> N <sub>2</sub> O <sub>2</sub>	C <sub>20</sub> H <sub>24</sub> N <sub>2</sub> O <sub>2</sub>	C <sub>13</sub> H <sub>14</sub> N <sub>2</sub> S <sub>2</sub>	C <sub>14</sub> H <sub>16</sub> N <sub>2</sub> S <sub>2</sub>
<i>Mr</i>	310.39	324.41	262.38	276.41
Crystal habit	block/colorless	block/colorless	block/colorless	block/colorless
Crystal system	tetragonal	monoclinic	monoclinic	orthorhombic
Space group	<i>P4<sub>3</sub>2<sub>1</sub>2</i>	<i>P2<sub>1</sub>/n</i>	<i>P2<sub>1</sub>/n</i>	<i>P2<sub>1</sub>2<sub>1</sub>2<sub>1</sub></i>
<i>a</i> /Å	5.823 (2)	8.061 (3)	8.425 (3)	8.0006 (5)
<i>b</i> /Å	5.823 (2)	8.412 (3)	16.564 (6)	10.2922 (6)
<i>c</i> /Å	51.22 (3)	13.493 (5)	10.324 (4)	17.8708 (8)
<i>α</i> /°	90.00	90.00	90.00	90.00
<i>β</i> /°	90.00	90.509 (5)	111.766 (5)	90.00
<i>γ</i> /°	90.00	90.00	90.00	90.00
<i>V</i> /Å <sup>3</sup>	1736.7 (13)	915.0 (6)	1338.1 (9)	1471.55 (14)
<i>Z</i>	4	2	4	4
<i>D</i> <sub>calc.</sub> /g·cm <sup>-3</sup>	1.187	1.178	1.302	1.248
<i>μ</i> /mm <sup>-1</sup>	0.08	0.08	0.38	0.35
<i>T</i> /K	293	293	298	293
<i>F</i> (000)	664	348	552	584
<i>R</i> <sub>int</sub>	0.109	0.070	0.041	0.028
<i>R</i> <sub>1</sub> [ <i>I</i> > 2σ( <i>I</i> )]	0.073	0.053	0.038	0.049
<i>wR</i> <sub>2</sub> /reflections	0.144/1527	0.136/1776	0.100/2620	0.134/2789
<i>S</i>	1.07	1.06	1.00	1.04

## 2.4 Computational Study

In this work, theoretical calculations were mainly used to investigate UV-Vis absorption properties of all six dimers.

In preliminary optimizations, the geometry of four dimers (**1**, **2**, **4** and **5**) were first extracted from their single-crystal X-ray structures and then optimized by employing density functional theory (DFT) method with the B3LYP exchange correlation functional calculations [27, 28] using 6-311+G(d,p) basis set. Geometry optimizations were computed in both the gas phase and ethanol solution (the same solvents as those in experiments, using conductor-like polarizable continuum model (CPCM) [29]). The absence of imaginary frequency in the calculated IR frequencies ensures that the optimized geometries correspond to true energy minima. The optimization of dimers **3** and **6** were carried out on the basis of similar dimers **2** and **5**, with bridging  $-(\text{CH}_2)_{12}-$  adopting all-anti conformations. All the subsequent calculations were performed based on optimized geometries. Vertical electronic excitations based on B3LYP/6-311+G(d,p) optimized geometries were computed using the time-dependent density functional

theory (TD-DFT) formalism [30] at the same level. UV-Vis spectra were done on the basis of the GaussView 5.0 package [31]. The major contributions of the transitions were designated with the aid of SWizard program [32] using the Gaussian distribution model with the half-bandwidth of  $500\text{ cm}^{-1}$  on the basis of TD-DFT results.

Relative atomic orbital contributions (mainly used in calculating alkyl C and H s/p orbital contributions) were obtained by natural bonding orbital (NBO) analysis of each particular frontier molecular orbital. NBO analysis was carried out on the file generated from the Gaussian option `pop=NBOread`, using version 5.0 of the Wisconsin NBO program [33].

All calculations were carried out using the Gaussian03 program package [34] on a Sunway BlueLight MPP supercomputer housed at the National Supercomputer Center in Jinan, China.

### 3. Results and Discussion

#### 3.1. NMR characterization and melting point

For all six dimers, the kinds of  $^1\text{H}$  NMR resonance peaks and the integration ratios were completely consistent with the formulation of the products, which can be assigned to “half-dimer”s, indicating that all dimers are symmetrical in the solution species and two “half-dimer”s are chemically equivalent on the NMR timescale. The simple  $^{13}\text{C}$  NMR spectra further confirm the symmetry feature of all dimers.

Another observed phenomenon is that the signals of the terminal groups do not seem to be affected by alkyl bridges. For example, the resonances of imine protons ( $\text{H}-\text{C}=\text{N}$ ) are at 8.25, 8.45, 8.22, 8.45, 8.44, and 8.42 ppm for dimers **1** to **6**, respectively. They are so close to each other that it's hard to distinguish them just on the point of chemical shift. Similarly, the resonances of the imine carbons are at 160.00, 159.99, and 159.52 ppm for dimers **1**, **2** and **3** in one same family; 154.65, 154.36 and 154.12 ppm for dimers **4**, **5** and **6** in another same family. The  $\delta$  values are almost the same if terminal groups are the same, regardless of different length linkers.

Dimers **1**, **2**, **4** and **5** have been reported before [16-22, 35], but there have been no single-crystal structural studies of them. Much of the earlier studies on different dimers leading to various properties are based on NMR spectra, and as a result, detailed structural information is often not available. What's more, there are many inconsistent statements about the same compound. As illustrative examples, the comparisons of NMR shifts in some literature are listed in **Tables. S1-S4**. For example, some differences

for the imine group and two methylene groups in dimer **1** were observed in the absorptions of the proton atoms which have signals at 8.22, 2.48, 1.88 ppm in literature [35a] and at 8.48, 3.76, 1.22 ppm in literature [16]; similarly in the absorptions of the carbon atoms which have signals at 161.6, 58.6, 32.4 ppm in literature [35a] and at 158.74, 58.42, 27.63 ppm in literature [16].

Besides NMR spectra, even the melting points are significantly different in some cases. For example, the melting point of dimer **4** is 68°C in literature [21], while 40-41°C in literature [22] and 36-38°C in literature [20]. The largest difference of melting point was observed in dimer **2**. According to literatures [13] and [14], the melting point should be 108-109°C or 105°C, whereas the melting point should be 116-117°C or 117-118°C according to literatures [16] and [19], but the result in our measurement is only 76.6-77.2°C, very similar to (nearly the same as) that of dimer **1** (76.4-77.6°C) and dimer **3** (76.8-77.0°C). Such an unusual similarity also occurs in another family of dimers **4**, **5** and **6**, with melting points of 63.9-64.3°C, 68.9-69.6°C and 59.8-60.3°C, respectively. It should be emphasized that the melting point cannot be reliably used to derive the molecular weight and the type of structural complexity.

The reason of so different characterization results lies in the difficulties to purify, which has been proven by two studies [35d, 35e]. Obviously, the quality of the data reported before does not allow for extensive discussions and precise crystal structure investigations are important.

## 3.2 Single-crystal X-ray crystallography

### 3.2.1. Crystal structure of **1**

Dimer **1** was first synthesized in 1963 [13, 35f] and thereafter it has been reported over 14 times. However the single-crystal structure has not been unambiguously determined till now. This dimer adopts  $C_2$  point-group symmetry and the  $C_2$  axis is parallel to the [1 1 0] direction through C9 atom. The asymmetric unit contains only one half-molecule and the two halves are really identical (Fig. 1a). As for the  $-\text{CH}_2-\text{CH}_2-\text{CH}_2-$  linker, **1** prefers gauche-gauche mode (abbreviated as g-g), which makes **1** twist and this mode may confer chirality to the dimer. But all dimers can be classified into two kinds of conformations, *i.e.* the two helical stereoisomers. So, although every dimer unit is chiral, the presence of dimer units with opposite chirality makes the crystal achiral.

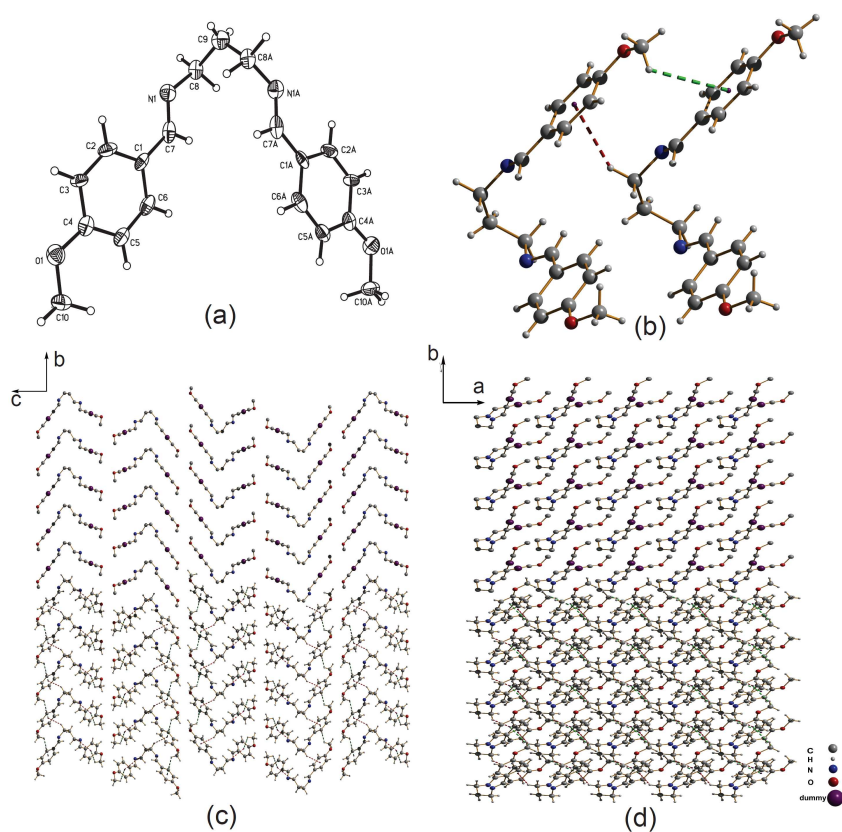


**Fig. 1.** (a) Atom numbered molecular structure of **1** with displacement ellipsoids for non-H atoms drawn at the 30% probability level at 293 K. “A” represents the symmetry code of “ $x, y, -z$ ”; (b) Two types of intermolecular C–H... $\pi$  H-bonds (C10–H6...Cg1<sup>( $x, 1+y, z$ )</sup> is shown with green dash lines and C8–H9...Cg1<sup>( $x, -1+y, z$ )</sup> with red dash lines). (c) Five layers (parallel to the crystallographic  $ab$  plane) formed by intermolecular C–H... $\pi$  H-bonds, view along the  $a$  axis, purposing to show the arrangement of repeated layers extending perpendicular to the  $c$  axis. The upper half is illustrated by the simplified dimers, which are obtained by substitution of benzene rings with their centers of gravity and omission of all hydrogen atoms. (d) One layer structure on the  $ab$  plane, purposing to show the same orientation of all dimers on the same plane. In fact, the picture is the projection of central layer in (c) on the  $ab$  plane.

In the packing structure of **1**, no classical hydrogen bond and valuable  $\pi$ - $\pi$  stacking interaction can be found and the dominant force is C–H... $\pi$  weak hydrogen bonding, which plays crucial role in the formation of  $g$ - $g$  conformation. The geometries of hydrogen bonds are listed in **Table S5**. As can be seen, there are two kinds of C–H... $\pi$  weak hydrogen bonds in **1**, one involves terminal methoxy group (C10–H6...Cg1<sup>( $x, 1+y, z$ )</sup>) and another involves linking methylene (C8–H9...Cg1<sup>( $x, -1+y, z$ )</sup>) (**Fig. 1b**). Each of the two interactions independently links **1** into the same 2D planes parallel to the crystallographic  $ab$  plane (**Fig. 1c** and **d**). No hydrogen bonds can be found between adjacent layers and packing of these layers in the crystal is stabilized only by van der Waals forces.

### 3. 2. 2. Crystal structure of 2

Dimer **2** contains crystallographic inversion symmetry ( $C_i$  point group) such that half molecule lies within the asymmetric unit. The inversion center lies between the center two C atoms (C9-C9A). As can be seen from **Fig. 2a**, dimer **2** maintains all-anti conformation as for the  $-(CH_2)_4$ -linking group.

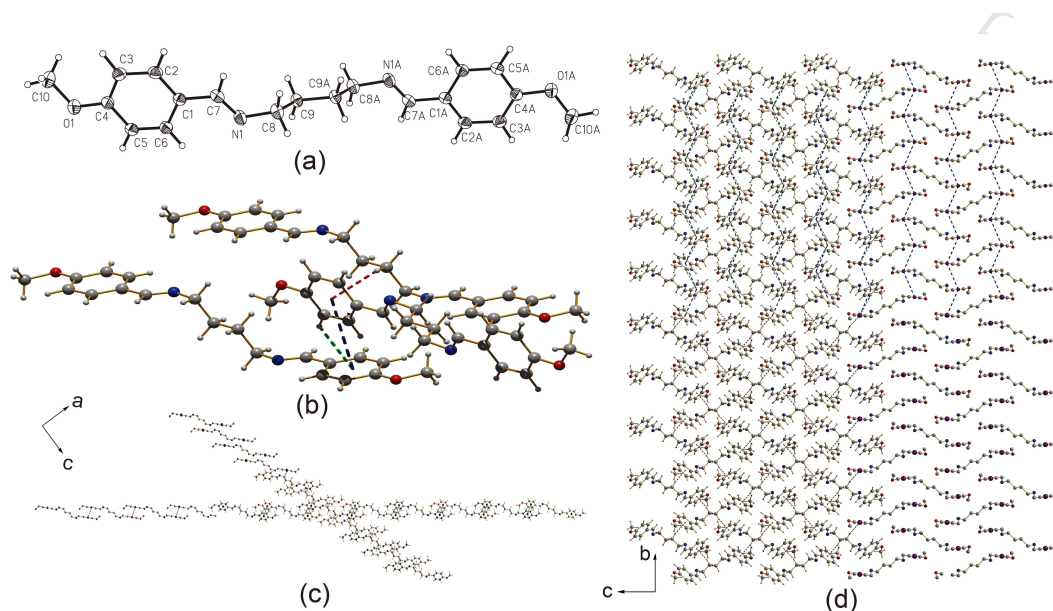


**Fig. 2.** (a) Atom numbered molecular structure of **2** with displacement ellipsoids for non-H atoms drawn at the 30% probability level at 293 K. Symmetry code of A:  $-x+1, -y+1, -z+2$ . (b) One kind of  $\pi, \pi$  -interactions (shown with blue dash lines) and two types of intermolecular C-H $\cdots\pi$  H-bonds (C3-H2 $\cdots$ Cg1<sup>(1/2-x, 1/2+y, 1/2-z)</sup> is shown with green dash lines and C9-H12 $\cdots$ Cg1<sup>(3/2-x, -1/2+y, 1/2-z)</sup> with red dash lines). (c) Two-dimensional structure formed by aforementioned intermolecular C-H $\cdots\pi$  H-bonds and  $\pi, \pi$  -interactions, view parallel to the spreading planes, *i.e.* the crystallographic  $(-1\ 0\ 1)$  (sloping) and  $(-1\ 0\ 3)$  (horizontal) planes. The left half and the upper half are illustrated by the simplified structures. (d) Three-dimensional structure formed by the aforementioned intermolecular C-H $\cdots\pi$  H-bonds and  $\pi, \pi$  -interactions, view along the  $a$  axis. The right half is illustrated by the simplified structures.

Similar as that in dimer **1**, no classical hydrogen bond can be found and two C-H $\cdots\pi$  weak hydrogen bonds play important role in the packing structure. Of the two C-H $\cdots\pi$  hydrogen bonds, one takes place between phenyl C-H and neighboring phenyl ring (C3-H2 $\cdots$ Cg1<sup>(1/2-x, 1/2+y, 1/2-z)</sup>) and another involves linking methylene (C9-H12 $\cdots$ Cg1<sup>(3/2-x, -1/2+y, 1/2-z)</sup>) (**Fig. 2b**). But different from that in dimer **1**, one kind of  $\pi$ - $\pi$  stacking interactions were found, which adopt edge-face geometry (**Fig. 2b**). The geometries of  $\pi, \pi$  -interactions and hydrogen bonds are listed in **Table S6** and **S7**, respectively. The first kind of C-H $\cdots\pi$  hydrogen bonds (C3-H2 $\cdots$ Cg1<sup>(1/2-x, 1/2+y, 1/2-z)</sup>) and  $\pi, \pi$  -interactions occur

simultaneously, both link dimer **2** into 2D layers parallel to the crystallographic  $(-1\ 0\ 3)$  plane (**Fig. 2c**). The second kind of C-H $\cdots\pi$  hydrogen bonds (C9-H12 $\cdots$ Cg1<sup>(3/2-x, -1/2+y, 1/2-z)</sup>) links **2** into another type of 2D layer framework with different orientations (parallel to the crystallographic  $(-1\ 0\ 1)$  plane) (**Fig. 2c**). Weaving of these layers in the crystal leads to the formation of 3D structure (**Fig. 2d**).

### 3. 2. 3. Crystal structure of **4**

X-ray structural analysis reveals that the asymmetric unit of **4** comprises of one complete dimer, and the C-C bonds in the  $-(\text{CH}_2)_3$ -linking chain assume a gauche-anti conformation (**Fig. 3(a)**).

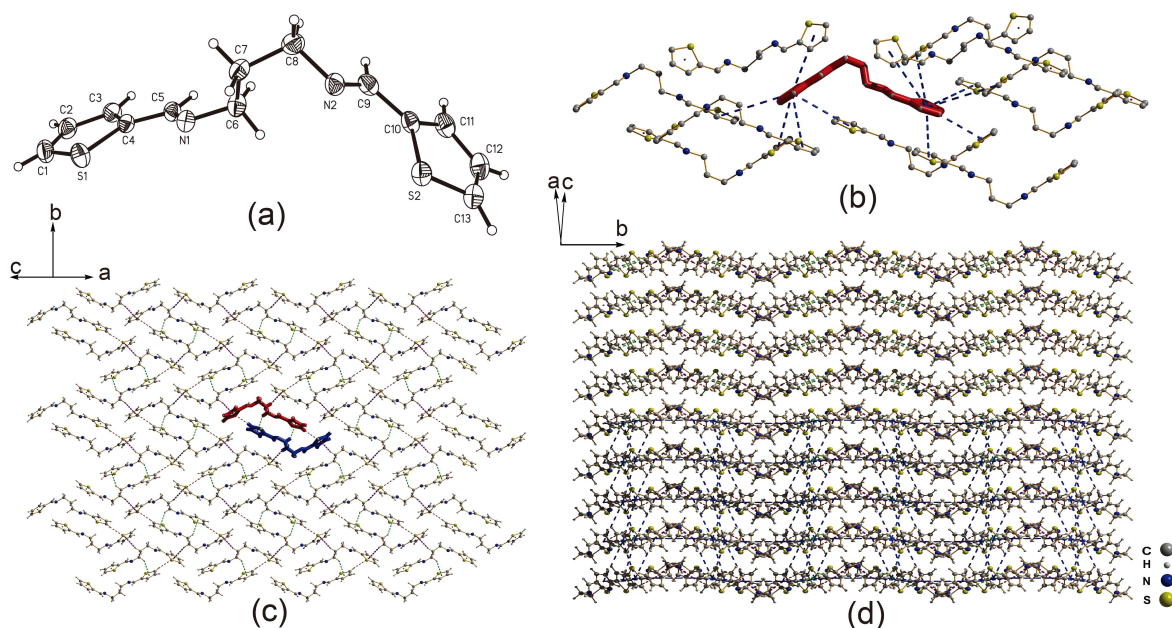


**Fig. 3.** (a) Atom numbered molecular structure of **4** with displacement ellipsoids for non-H atoms drawn at the 30% probability level at 298 K. (b) One dimer (the highlighted red one) is surrounded by ten dimers illustrating the seven kinds of  $\pi, \pi$ -interactions (shown with blue dash lines). All hydrogen atoms are omitted for clarity. (c) 2D structure formed by three types of intermolecular C-H $\cdots\pi$  H-bonds, view perpendicular to the lying plane, *i.e.*  $(1\ 0\ 1)$  crystal face. The highlighted red and blue dimers in the center constitute a large dimer through two types of intermolecular C-H $\cdots\pi$  H-bonds (C1-H1 $\cdots$ Cg2<sup>(1-x, -y, 1-z)</sup> is shown with red dash lines and C6-H6 $\cdots$ Cg1<sup>(1-x, -y, 1-z)</sup> with green dash lines). (d) Crystal packing diagram for dimer **4** viewed along  $[3\ 0\ -4]$  direction. The upper four layers contain only three types of intermolecular C-H $\cdots\pi$  H-bonds, and the lower five layers contain all kinds of interactions, including three types of intermolecular C-H $\cdots\pi$  H-bonds and seven kinds of  $\pi, \pi$ -interactions.

There are seven kinds of  $\pi, \pi$ -interactions in the supramolecular structure of **4** (**Fig. 3b**) and the geometries are listed in **Table S8**. As we can see, six kinds of them adopt edge-face geometries and one

offset mode. The geometries of three kinds of C–H... $\pi$  H-bonds are listed in **Table S9**. The first one (C1–H1...Cg2<sup>(1-x, -y, 1-z)</sup>) is between thiophene C–H and neighboring thiophene ring, and the other two involve alkyl bridge. Interestingly, the first and the second (C6–H6...Cg1<sup>(1-x, -y, 1-z)</sup>) kinds of C–H... $\pi$  H-bonds independently link dimer **4** into the same large dimer (**Fig. 3c**). Meanwhile, the third (C7–H7...Cg2<sup>(1/2+x, 1/2-y, -1/2+z)</sup>) kind of C–H... $\pi$  H-bonds links dimer **4** into an infinite zigzag chain extending along the [3 0 -4] direction. If all three C–H... $\pi$  H-bonds are considered, the neighboring dimers are connected to give 2D layers extending along (1 0 1) crystal face (**Fig. 3c** and **3d**). These layers are further bridged by  $\pi$ ,  $\pi$ –interactions to afford a 3D framework (**Fig. 3d**). It should be noted that  $\pi$ ,  $\pi$ –interactions also exist inside the layers.

### 3. 2. 4. Crystal structure of **5**

In dimer **5**, a full dimer constitutes the content of the asymmetric unit, but the two center methylene groups in the alkyl bridge exhibit conformational disorder ( $m = 0.53$ ) over two sets of positions. Interestingly, one set exhibits anti-gauche-anti conformation (**Fig. 3a**) and another adopts all-anti conformation, which proves that the energy barrier separating these two kinds of conformations is very low.

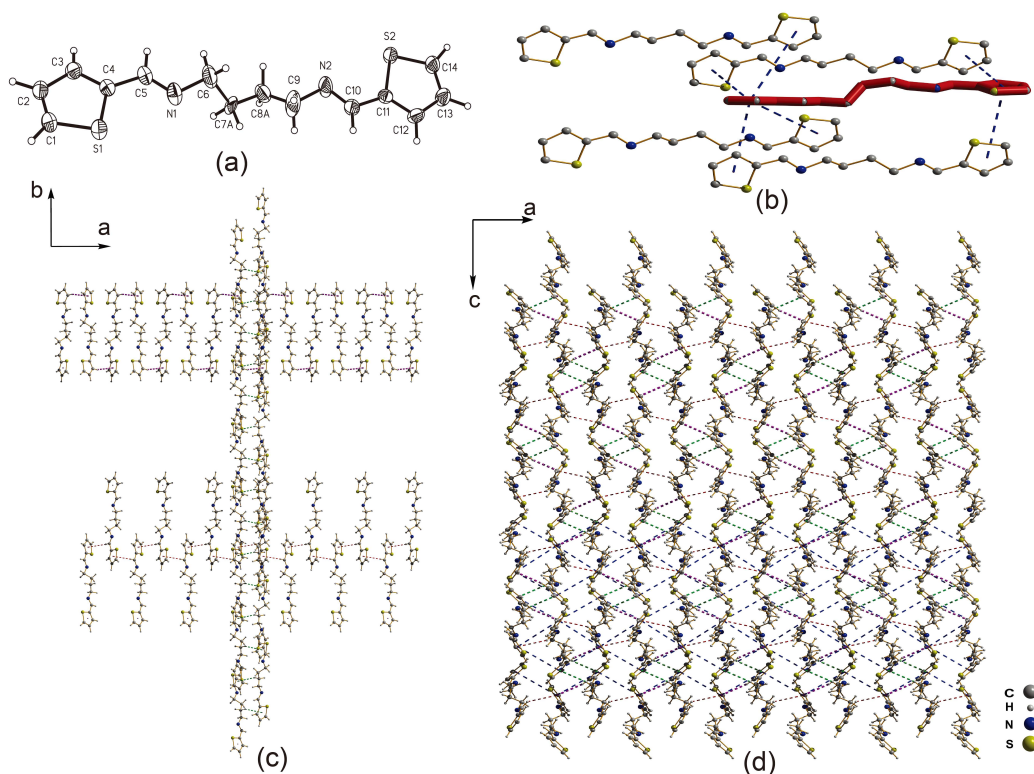


**Fig. 4.** (a) Atom numbered molecular structure of **5** with displacement ellipsoids for non-H atoms drawn at the 30% probability level at 293 K. The disordered parts of C7A and C8A (i.e. C7B and C8B) have been omitted for clarity. (b)

One dimer (the highlighted red one) is surrounded by four dimers illustrating the three kinds of  $\pi, \pi$ -interactions (shown with blue dash lines). All hydrogen atoms are omitted for clarity. (c) Three types of intermolecular C-H $\cdots\pi$  H-bonds are illustrated with three kinds of color dash lines, which help dimer **5** link into chains with two orientations: one oriented along *b* axis and two along *a* axis, viewed along *c* axis. (d) Crystal packing diagram for dimer **5** viewed along *b* axis. The upper half contains only three types of intermolecular C-H $\cdots\pi$  H-bonds, and the lower half contains all kinds of interactions, including three types of intermolecular C-H $\cdots\pi$  H-bonds and three kinds of  $\pi, \pi$ -interactions.

Similar as that in dimers **2** and **4**,  $\pi, \pi$ -interactions and C-H $\cdots\pi$  weak hydrogen bonds work together to help link dimer **5** molecules into 3D crystal. All three kinds of  $\pi, \pi$ -interactions adopt edge-face geometries (Fig. 3b and Table S10), leading to the formation of a 2D layer structure parallel to the *ab* plane. Each kinds of these three C-H $\cdots\pi$  weak hydrogen bonds resulting in the formation of 1D chains with parallel and perpendicular orientations (Fig. 3c and Table S11). Instead, all of them work together to give a complicated 3D hydrogen-bonded network (Fig. 3d).

In conclusion, similar dimers **1** and **2** form colorless crystals in the space groups  $P4_32_12$  (No. 96) and  $P2_1/n$  (No. 14), while another set of similar dimers **4** and **5** form colorless crystals in  $P2_1/n$  (No. 14) and  $P2_12_12_1$  (No. 16), respectively. This illustrates the flexible nature of these dimers in forming a variety of different packing motifs. As for non-covalent interactions, no classical hydrogen bond can be found in these four dimers, C-H $\cdots\pi$  hydrogen bonding and  $\pi - \pi$  stacking interactions help to form interesting 1D, 2D and even 3D supramolecular arrays.

### 3.3 Comparison of UV-Vis absorption spectra of six dimers experimentally and theoretically

The observed electronic absorption spectra of six dimers ( $10^{-5}$  mol·L $^{-1}$  solution in ethanol) are shown in Fig. 5. It can be seen that similar dimers **1**, **2** and **3** have nearly the same spectra, and the phenomena also occurs in another set of similar dimers **4**, **5** and **6**. That is to say, the lengthening of the alkyl bridge has no effect on the UV-Vis spectra. In order to further analyze the result from the point of molecular structure, and to determine the spectroscopy mechanisms, theoretical calculations were performed to make the assignment of these electronic transitions.

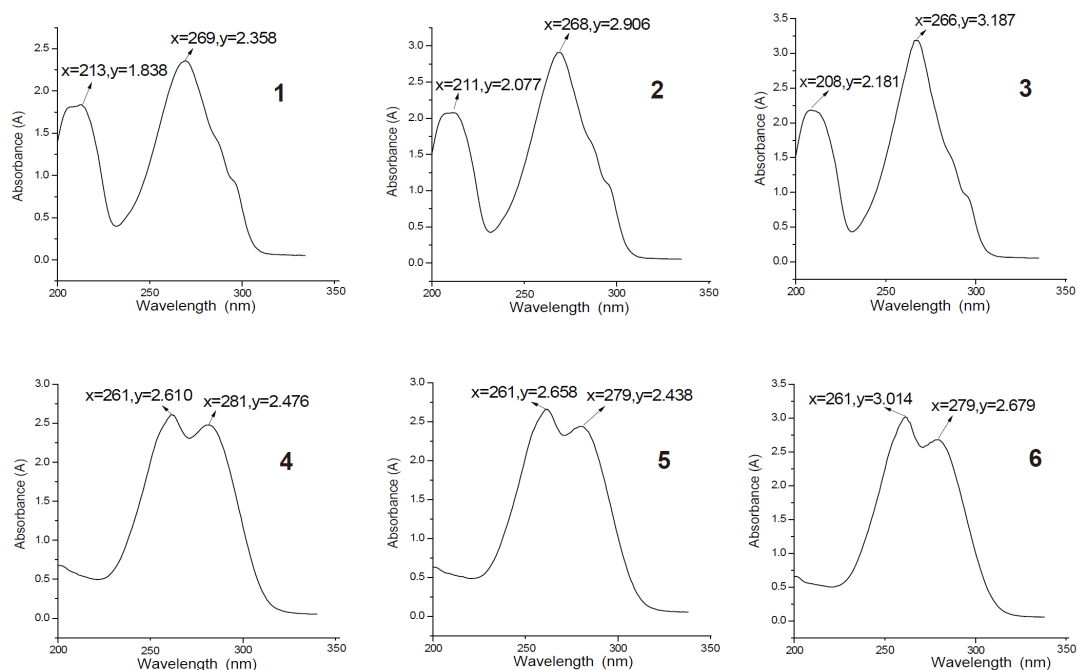


**Fig. 5** UV-Vis spectra of the six dimers.

The geometries of dimers **1**, **2**, **4** and **5** used for calculations were derived from their single-crystal X-ray structures. The optimized geometrical images and their single-crystal X-ray structures have the same conformations and the same point groups. But the crystal structures of dimers **3** and **6** have not been obtained, and as a result, detailed conformations of the molecules are not available. In order to shed more light on the precise similarities/differences in the UV-Vis spectra between different kinds of conformations, similar calculations (only in ethanol solution) were performed for dimers **1**, **4** and **5** in their all-anti conformations, which are often be considered as the most stable kind of conformation. The calculated UV-Vis spectra are shown in **Fig. S19**. A summary of our results as follows: 1) Comparisons of (a) and (b), (d) and (e), (f) and (g), (i) and (j) in **Fig. S19** show that the spectra calculated in gas phase and ethanol solution are similar, with small deviations all less than 10 nm; 2) Comparisons of (b) and (c), (g) and (h), (j) and (k) in **Fig. S19** show that the spectra calculated in crystal molecular conformation and all-anti conformation are remarkably similar, with small deviations all less than 5 nm; 3) Comparisons of UV-Vis spectra in **Fig. 5** and **Fig. S19** show that calculated results are all in line with experimental data for four dimers, which represents two different families of dimers. These results provoked us to further calculate the UV-Vis spectra of dimers **3** and **6**, though no detailed conformations are available.

Calculations of the UV-Vis spectra of dimers **3** and **6** were performed only in ethanol solution with all-anti conformations. The results are diagrammed in **Fig. S20**. Obviously, the calculated spectra

correctly reproduced the experimental results and the degree of match-up is so good that their electronic structures can be analyzed for in-depth understanding of their UV-Vis spectra. The following analyses are mainly based on the ethanol solution, in which the lowest 60 singlet - singlet spin-allowed excitation states (all up to an energy of ~6.9 eV or ~180 nm) were taken into account for all calculations.

Excitation energies, oscillator strengths and corresponding electronic transition compositions for the simulated absorption bands of dimers **1-6** are listed in **Table S12**. Within the near UV-Vis range, the strongest absorption oscillator strengths are found at 223.0 and 279.0; 223.4 and 280.0; 253.1 and 295.0; 251.9 and 285.1; 223.2 and 277.1; 251.6 and 282.4 nm respectively. On the basis of these calculated match-up results, the transition mechanisms can be interpreted.

According to **Table S12**, the observed bands of dimer **1** at 213.0 and 269.0 nm correspond to the calculated absorption bands at 223.0 and 279.0 nm, respectively. The former is dominated by the transition from HOMO-4 to LUMO+1 (75%) and the latter is dominated by the transition from HOMO-1 to LUMO+1 (69%). Molecular orbitals (MOs) in **Figs. S21** and **S22** show that HOMO-4 entirely localizes on benzene rings, while HOMO-1 and LUMO+1 mainly localize on benzene rings and imine bonds. So the two UV-Vis absorption bands should be characterized by  $\pi \rightarrow \pi^*$  transitions. Dimer **1** adopts  $C_2$  point-group symmetry with a twofold axis splitting the molecule into two identical halves, so do the MOs. It should be mentioned that most HOMOs and LUMOs involved in the transitions mainly localize on benzene rings and imine bonds, having little or nothing to do with the alkyl bridge. HOMO-2 and HOMO-3 may be two exceptions, but they do not participate in the transitions that contribute to the band at 223.0 nm. That's why the corresponding calculated absorption band move only 1.4 nm (from 223.0 to 224.4 nm) when the bridging  $-(CH_2)_3-$  conformations change from g-g to anti-anti mode (abbreviated as a-a). Another band at 279.0 nm moves to 284.7 nm when the bridge conformations change, probably due to HOMO-2 and HOMO-3, though their contributions are small (13% and 8%, respectively).

Similarly, dimer **2** ( $C_i$  point group) has two observed bands at 211.0 and 268.0 nm, corresponding to the calculated absorption bands at 223.4 and 280.0 nm, respectively. The main absorptions arise from the HOMOs of HOMO-5, HOMO-4, HOMO-1, HOMO, to LUMOs of LUMO, LUMO+1, LUMO+2, LUMO+3. These MOs in **Figs. S23** and **S24** have similar predominant character, i.e. almost entirely localize on benzene rings and imine bonds, having little or nothing to do with the alkyl bridge, apparently indicating  $\pi \rightarrow \pi^*$  transitions.

Dimer **3** has the same terminal groups as dimers **1** and **2**, so they have similar observed/calculated absorption bands. The MO structures are shown in **Figs. S25** and **S26**, still mainly localizing over benzene rings mixed with C=N bonds. Therefore, the two bands can also be assigned as the  $\pi \rightarrow \pi^*$  transitions.

Dimers **4**, **5** and **6** have different terminal groups from those in dimers **1**, **2** and **3**, so they have another kind of UV-Vis spectra containing two strong peaks above 200 nm, one around 261 nm and another around 280 nm. The calculated absorption bands are between 252-253 nm and 282-295 nm, respectively (**Table S12**).

The band around 261.0 nm of dimer **4** is dominated by the electron excitations from HOMO-3/HOMO-2 to LUMO/LUMO+1. The distributions of the electronic states in these MOs can be seen in **Fig. S27**, where HOMO-3 and HOMO-2 have very similar character (in fact, they are quasi-degenerated orbitals with nearly the same energy, *i.e.* -0.26813 and -0.26784 a.u. respectively) localizing over one terminal thiophene ring. Interestingly, LUMO and LUMO+1 also have very similar character (in fact, they are also quasi-degenerated orbitals with nearly the same energy, *i.e.* -0.06855 and -0.06419 a.u. respectively) mainly lie over terminal thiophene rings and C=N bonds. Apparently, this band is originated from  $\pi \rightarrow \pi^*$  transitions. Another band at 281.0 nm uncommonly arises from single electron excitations from HOMO to LUMO. **Fig. S28** and NBO analysis show that HOMO is localized over the entire dimer, including thiophene rings (around 71.68%), C=N bonds (around 22.18%) and bridging  $-(\text{CH}_2)_3-$  groups (around 6.14%), while LUMO is localized on the terminal thiophene rings and C=N bonds. To some extent, this band is largely originated from  $\pi \rightarrow \pi^*$  transitions mixed with few  $\sigma \rightarrow \pi^*$  transitions.

The transition mechanism of the band around 261.0 nm of dimer **5** is nearly the same as that in dimer **4**. As the initial states, the high-lying occupied orbitals (HOMO-3 and HOMO-2) are degenerated orbitals with the same energy (-0.26794 a.u.), and completely contributed by thiophene rings. LUMO and LUMO+1 orbitals (the final states of the transition) are quasi-degenerated orbitals with nearly the same energy, *i.e.* -0.06616 and -0.06593 a.u. respectively, mainly localizing over terminal thiophene rings and C=N bonds (**Fig. S29**). Accordingly, this band represents  $\pi \rightarrow \pi^*$  transitions. Another band of dimer **5** is at 279.0 nm, arising from four kinds of transitions (**Table S12** and **Fig. S30**). But the most important transitions are from HOMO-1/HOMO to LUMO/LUMO+1 (41% + 41%). Both the initial states and the final states are quasi-degenerated orbital; both mainly localize over the terminal thiophene

rings and C=N bonds, mixed with minor parts of the alkyl bridge. So, this band is largely originated from  $\pi \rightarrow \pi^*$  transitions mixed with some  $\sigma \rightarrow \pi^*$  transitions.

The transition mechanism of dimer **6** is nearly the same as that in dimer **4** and **5**. In brief, the band observed at 261.0 nm, corresponding to the calculated band at 251.6 nm, can be assigned as the  $\pi \rightarrow \pi^*$  transitions and have nothing to do with the alkyl bridge (**Table S12** and **Fig. S31**). The band observed at 279.0 nm, corresponding to the calculated band at 282.4 nm, is largely originated from the  $\pi \rightarrow \pi^*$  transitions mixed with minor parts of some  $\sigma \rightarrow \pi^*$  transitions (**Table S12** and **Fig. S32**).

All together our data, the absorption spectra reproduced from DFT calculations fit the experimental results well, so attempts to understand the nature of electronic transitions were carried out through comparison. Two important notes: 1) This two series of dimers provides longer alkyl bridges between two methoxy benzene rings and two thiophene rings (propane  $\rightarrow$  butane  $\rightarrow$  dodecane), while maintaining nearly the same UV-Vis spectra; 2) All six dimers have two main absorption bands, which can be assigned as the  $\pi \rightarrow \pi^*$  transitions and have little or nothing to do with the alkyl bridges, so the lengthening and the conformations of alkyl bridges have small effect on UV-Vis spectra.

### 3.4 Luminescent properties of six dimers

The luminescent spectra of six dimers have been investigated in ethanol solution at room temperature (**Fig. 6**). Dimers **1**, **2** and **3** display one similar emission band around 437 nm, while dimers **4**, **5** and **6** display two similar emission bands around 408 and 436 nm. Not only the emission wavelength, but also the profiles of these spectra are quite similar. Our attempt to rationalize their fluorescence mechanisms and to explain the similarities in their experimental observations by DFT calculations failed. It is postulated that the emission bands of the dimers should be ascribed to the intraligand  $\pi^*-\pi$  charge transfer and have little or nothing to do with the alkyl bridges, and the overall  $\pi$ -electron densities of the electronic excited states are barely delocalized in these whole dimers.

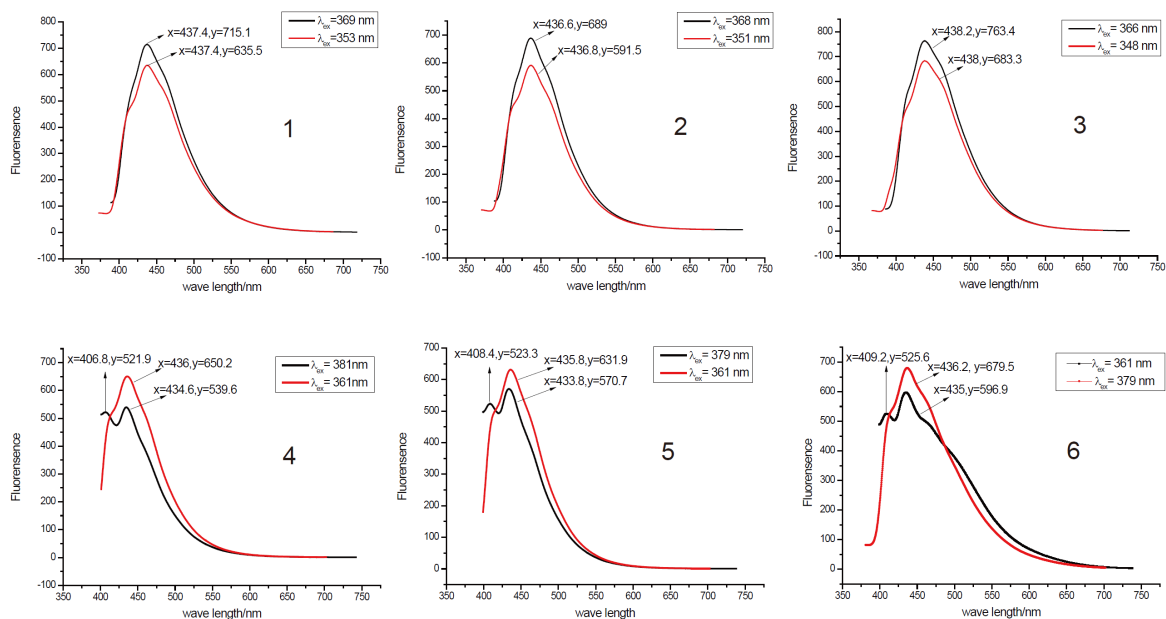


**Fig. 6** Fluorescence emission spectra of the six dimers ( $5 \times 10^{-5}$  mol·L<sup>-1</sup> solution in ethanol, room temperature).

#### 4. Conclusions

We have prepared two families of alkyl-linked Schiff-base dimers containing  $\pi$ -conjugated terminal groups. On the basis of both experimental results and nicely fitted theoretical reproduction we believe that the following conclusions can be made about the structure, non-covalent bonding, and optical properties of similar dimers containing bridging alkyl and aryl terminal.

Single crystal structures of four out of six dimers were determined. The results showed that no correlation occurs between the crystal structure and the mode of weak interaction patterns, even though they have similar molecule structures. For example, similar dimers **1** and **2** crystallize in the space groups  $P4_32_12$  (No. 96) and  $P2_1/n$  (No. 14), while another set of similar dimers **4** and **5** form crystals in  $P2_1/n$  (No. 14) and  $P2_12_12_1$  (No. 16), respectively. After all, they have similar non-covalent interactions (no classical hydrogen bonding, only weak C–H $\cdots\pi$  hydrogen bonds and  $\pi$ – $\pi$  stacking interactions) and similar molecule structures.

The profiles of UV-Vis and luminescent spectra of every family were quite similar to each other, indicating the optical properties related to the electronic transition have little or nothing to do with the alkyl bridges, which can be justified by TD-DFT calculations. Theoretical reproduction reveals that all main absorption bands should be predominately assigned as the  $\pi \rightarrow \pi^*$  transitions and the electronic structures of frontier orbitals are not disturbed by the alkyl bridges. So the lengthening and the

conformations of alkyl bridges have small effect on UV-Vis spectra. Thus, this study provides a better understanding of the role that alkyl linking groups can play in the changing of photophysical and electronic properties of dimers. Namely, these properties of the materials can be rationally predicted and relatively straightforward to determine.

## 5. Acknowledgments

The authors are thankful to the Science & Technology Development Projects of Shandong Province in China (No. 2011GGX10706 and 2012GGX10702) and the National Natural Science Foundation of PR China (NSFC, No. 21103100) for financial support. Generous support in computing resources from the National Supercomputer Center in Jinan, China, is greatly appreciated.

## Supplementary Material

Supplementary Information available: **Tables S1 – S12, Figures S1 – S32** mentioned in the text. Crystallographic information files of five compounds. CCDC < 1528884, 1528885, 1528887 and 1528886 > contains the supplementary crystallographic data for < **1**, **2**, **4** and **5** >. These data can be obtained free of charge from The Cambridge Crystallographic Data Centre via [http://www.ccdc.cam.ac.uk/data\\_request/cif](http://www.ccdc.cam.ac.uk/data_request/cif), or from the Cambridge Crystallographic Data Centre, 12 Union Road, Cambridge CB2 1EZ, UK; fax: (+44) 1223-336-033; or e-mail: [deposit@ccdc.cam.ac.uk](mailto:deposit@ccdc.cam.ac.uk).

## References and notes

- [1] G. Berube, *Current Medicinal Chemistry*, 13 (2006) 131-154.
- [2] P.S. Portoghese, *J. Med. Chem.* 35 (1992) 1927-1937.
- [3] (a) T.A. Hill, S.G. Stewart, S.P. Ackland, J. Gilbert, B. Sauer, J. A. Sakoff and A. McCluskey. *Bioorg. Med. Chem.* 15 (2007) 6126-6134;  
(b) S. S. Cheng, Y. Shi, X. N. Ma, D. X. Xing, L. D. Liu, Y. Liu, Y. X. Zhao, Q. C. Sui, X. J. Tan, *J. Mol. Struct.* 1115 (2016) 228-240.
- [4] (a) D. Bagnis, L. Beverina, H. Huang, F. Silvestri, Y. Yao, H. Yan, G. A. Pagani, T. J. Marks, A. Facchetti, *J. Am. Chem. Soc.* 132 (2010) 4074–4075;  
(b) L. Ding, H. Li, T. Lei, H. Ying, R. Wang, Y. Zhou, Z. Su, J. Pei, *Chemistry of Materials*, 24 (2012) 1944-1949;  
(c) O. Ostroverkhova, *Chem. Rev.* 116 (2016) 13279–13412 and references therein.
- [5] F. Würthner, T. E. Kaiser, and C. R. Saha-Möller, *Angew. Chem. Int. Ed.* 50 (2011) 3376 – 3410.
- [6] (a) D. A. Fowler, J. L. Atwood, G. A. Baker, *Chem. Commun.* 49 (2013) 1802-1804;

- (b) R. Boese, H. C. Weiss, D. Bläser, *Angew. Chem., Int. Ed.* 38 (1999) 988–992;
- (c) K. Avasthi, S. M. Farooq, R. Raghunandan, P. R. Maulik, *J.Mol.Struct.*, 927 (2009) 27-36;
- (d) O. Kretschmann, S. W. Choi, M. Miyauchi, I. Tomatsu, A. Harada, and H. Ritter, *Angew. Chem. Int. Ed.* 45(2006) 4361–4365;
- (e) P. A. Gale, K. Navakhun, S. Camiolo, M. E. Light and M. B. Hursthouse, *J. Am. Chem. Soc.* 124 (2002) 11228–11229.
- [7] (a) D. A. Fowler, C. R. Pfeiffer, S. J. Teat, G. A. Baker, and J. L. Atwood, *Cryst. Growth Des.* 14 (2014) 4199–4204;
- (b) R. S. Patil, H. Kumari, C. L. Barnes and J. L. Atwood, *Chem. Commun.* 51 (2015) 2304-2307;
- (c) H. Kumari, A. J. Good, V. J. Smith, L. J. Barbour, C. A. Deakyne and J. L. Atwood, *Supramol. Chem.*, 25 (2013) 591–595;
- (d) I. Ling, A. N. Sobolev, K. Sabah and R. Hashim, *CrystEngComm*, 17 (2015) 5841–5848.
- [8] M. Morisue, Y. Hoshino, M. Nakamura, T. Yumura, S. Machida, Y. Ooyama, M. Shimizu, and J. Ohshita, *Inorg. Chem.* 55 (2016) 7432–7441.
- [9] M. T. Trinh, Y. Zhong, Q. Chen, T. Schiros, S. Jockusch, M. Y. Sfeir, M. Steigerwald, C. Nuckolls, X. Zhu, *J. Phys. Chem. C* 119 (2015) 1312–1319.
- [10] (a) T. C. Berkelbach, M. S. Hybertsen, D. R. Reichman, *J. Chem. Phys.* 2013, 138 (2013) 114103;
- (b) J. Zirzmeier, D. Lehnerr, P. B. Coto, E. T. Chernick, R. Casillas, B. S. Basel, M. Thoss, R. R. Tykwinski, D. M. Guldi, *Proc. Natl. Acad. Sci. U. S. A.* 112 (2015) 5325–5330;
- (c) T. Sakuma, H. Sakai, Y. Araki, T. Mori, T. Wada, N. V. Tkachenko, T. Hasobe, *J. Phys. Chem. A*, 120 (2016), 1867–1875.
- [11] O. Varnavski, N. Abeyasinghe, J. Aragón, J. J. Serrano-Pérez, E. Ortí, J. T. López Navarrete, K. Takimiya, D. Casanova, J. Casado, T. Goodson, *J. Phys. Chem. Lett.* 6 (2015) 1375–1384.
- [12] M. C. Yoon, S. Lee, S. Tokuji, H. Yorimitsu, A. Osuka and D. Kim, *Chem. Sci.* 4 (2013) 1756-1764.
- [13] J. H. Billman, J. L. Meisenheimer, *J. Med. Chem.* 6(1963) 682-683.
- [14] K. N. Zelenin, V. V. Alekseyev, I. V. Ukrantsev, I. V. Tselinsky, *Org. Prep. Proced. Int.* 30 (1998) 53–61.
- [15] J. M. Locke, R. Griffith, T. D. Bailey, R. L. Crumbie, 65(2009), 10685-10692.
- [16] S. Alina, S. Cristian, K. Tadeshige, N. Satoko, M. Yoshiharu, Y. Tomoko, M. Keisuke, T. Masashi, *J. Chem. Soc., Perkin Trans. 1* (2001) 2071–2078.
- [17] M. S. Singh, A. K. Singh, Pratibha Singh & Ruchi Jain, *Organic Preparations and Procedures International: The New Journal for Organic Synthesis*, 37(2005) 173-177.

- [18] H. Temel, Ü. Cakir, H. İ. Uğras, *Russ. J. Inorg. Chem.* 46(2001) 1846-1850.
- [19] Y. Goek, E. Cetinkaya, *Turk. J. Chem.* 28(2004), 157-162.
- [20] R. K. Y. Ho, S. E. Livingstone, *Aust. J. Chem.* 18(1965), 659-671.
- [21] L. N. Khokhlova, S. Germane, N. P. Erchak, and É. Lukevits, *Chem. Heterocycl. Com.*, 30(1994) 279-282.
- [22] T. Poursaberi, L. Hajiagha-Babaei, M. Yousefi, S. Rouhani, M. Shamsipur, M. Kargar-Razi, A. Moghimi, H. Aghabozorg and M.R. Ganjali, *Electroanal.* 13 (2001) 1513–1517.
- [23] G. M. Sheldrick, SADABS, Bruker AXS Inc., Madison, Wisconsin, USA, 2004.
- [24] G. M. Sheldrick, *Acta Crystallogr. Sect. A*, 64 (2008) 112-122.
- [25] Bruker APEX II (version 2.0-1), SAINT (version 7.23A), XPREP (version 2005/2), SHELXTL (version 6.1). Bruker AXS Inc., Madison, Wisconsin, USA, 2005.
- [26] K. Brandenburg, H. Putz, DIAMOND. Crystal Impact GbR, Bonn, Germany, 2005.
- [27] A.D. Becke, *J. Chem. Phys.* 98 (1993) 5648-5652.
- [28] C. Lee, W. Yang, R.G. Parr, *Phys. Rev. B: Condens. Matter Mater. Phys.* 37 (1988) 785-789.
- [29] (a) V. Barone, M. Cossi, *J. Phys. Chem. A*, 102 (1998) 1995–2001;  
(b) M. Cossi, N. Rega, G. Scalmani, V. Barone, *J. Comput. Chem.* 24 (2003) 669–681;  
(c) Y. Takano, K. Houk, *J. Chem. Theory. Comput.* 1 (2005) 70–77.
- [30] (a) R. Bauernschmitt, R. Ahlrichs, *Chem. Phys. Lett.* 256 (1996) 454-464;  
(b) R. E. Stratmann, G. E. Scuseria, M. J. Frisch, *J. Chem. Phys.* 109 (1998) 8218-8224;  
(c) M. E. Casida, C. Jamorski, K. C. Casida, D. R. Salahub, *J. Chem. Phys.* 108 (1998) 4439-4449.
- [31] A. B. Nielsen, A. J. Holder, *GaussView, User's Reference*, GAUSSIAN, Inc.: Pittsburgh, PA, USA **1997-1998**.
- [32] (a) S. I. Gorelsky, *SWizard Program* Revision 4.6; University of Ottawa: Ottawa, Canada, **2010**;  
<http://www.sg-chem.net/>.  
(b) S. I. Gorelsky, A. B. P. Lever, *J. Organomet. Chem.* 635 (2001) 187-196.
- [33] NBO 5.0; E. D. Glendening, J. K. Badenhoop, A. E. Reed, J. E. Carpenter, J. A. Bohmann, C. M. Morales, F. Weinhold, Theoretical Chemistry Institute, University of Wisconsin, Madison, WI, 2001.
- [34] M. J. Frisch, G. W. Trucks, H. B. Schlegel, G. E. Scuseria, M. A. Robb, J. R. Cheeseman, J. A. Jr. Montgomery, T. Vreven, K. N. Kudin, J. C. Burant, J. M. Millam, S. S. Iyengar, J. Tomasi, V. Barone, B. Mennucci, M. Cossi, G. Scalmani, N. Rega, G. A. Petersson, H. Nakatsuji, M. Hada, M. Ehara, K. Toyota, R. Fukuda, J. Hasegawa, M. Ishida, T. Nakajima, Y. Honda, O. Kitao, H. Nakai, M. Klene, X. Li, J. E. Knox, H. P. Hratchian, J. B. Cross, V. Bakken, C. Adamo, J. Jaramillo, R. Gomperts, R. E. Stratmann, O. Yazyev, A.

- J. Austin, R. Cammi, C. Pomelli, J. W. Ochterski, P. Y. Ayala, K. Morokuma, G. A. Voth, P. Salvador, J. J. Dannenberg, V. G. Zakrzewski, S. Dapprich, A. D. Daniels, M. C. Strain, O. Farkas, D. K. Malick, A. D. Rabuck, K. Raghavachari, J. B. Foresman, J. V. Ortiz, Q. Cui, A. G. Baboul, S. Clifford, J. Cioslowski, B. B. Stefanov, G. Liu, A. Liashenko, P. Piskorz, I. Komaromi, R. L. Martin, D. J. Fox, T. Keith, M. A. Al-Laham, C. Y. Peng, A. Nanayakkara, M. Challacombe, P. M. W. Gill, B. Johnson, W. Chen, M. W. Wong, C. Gonzalez, J. A. Pople, *Gaussian 03*, revision C.02; Gaussian, Inc.: Wallingford, CT, **2004**.
- [35] (a) I. L. Paiva, G. S. G. de Carvalho, A. D. da Silva, P. P. Corbi, F. R. G. Bergamini, A. L. B. Formiga, R. Diniz, W. R. do Carmo, C. Q. F. Leite, F. R. Pavan, A. Cuin, *Polyhedron* **62** (2013) 104–109;
- (b) M. R. Ganjali, T. Poursaberi, L. H. Babaei, S. Rouhani, M. Yousefi, M. Kargar-Razi, A. Moghimi, H. Aghabozorg, M. Shamsipur, *Analytica Chimica Acta*, **440**(2001) 81–87;
- (c) M. R. Ganjali, F. Basiripour, M. Shamsipur, O. R. Hashemi, A. Moghimi & H. Aghabozorg, *Int. J. Environ. An. Ch.* **83** (2003) 997-1008;
- d) A. P. Molchanov, D. I. Sipkin, Yu. B. Koptelov, and R. R. Kostikov, *Russ. J. Org. Chem.* **37**(2001) 841-851;
- e) M. R. A. Pillai, C. L. Barnes, C. S. John, D. E. Troutner, and E. O. Schlemper, *Journal of Crystallographic and Spectroscopic Research*, **23**(1993) 949-953;
- f) H. Y. Cheng, C. Chen, I. F. Chien, P. C. Kan, H. L. Chin, S. H. Hsiao, P. J. Shao, *Yaoxue Xuebao*, **10**(1963) 407-417.

**Keywords:** alkyl-bridge, bis(imido) symmetrical Schiff bases, crystal structure, optical properties, DFT calculations.

**Highlights:**

- Single crystal structures of 4 out of 6 dimers were determined.
- UV-Vis and luminescent properties have been evaluated.
- DFT/B3LYP/6-311+G(d,p) method was employed to interpret optical properties.
- The effects of varying bridging length appended on dimers were explored.